Bioconjugate Chemistry

Article

pubs.acs.org/bc

In Vivo Imaging of Multidrug Resistance Using a Third Generation MDR1 Inhibitor

Melissa M. Sprachman,[†] Ashley M. Laughney,[†] Rainer H. Kohler,[†] and Ralph Weissleder*[,†,‡]

[†]Center for Systems Biology, Massachusetts General Hospital, 185 Cambridge Street, CPZN 5206, Boston, Massachusetts 02114, United States

[‡]Department of Systems Biology, Harvard Medical School, 200 Longwood Avenue, Boston, Massachusetts 02115, United States

Supporting Information

ABSTRACT: Cellular up-regulation of multidrug resistance protein 1 (MDR1) is a common cause for resistance to chemotherapy; development of third generation MDR1 inhibitors—several of which contain a common 6,7-dimethoxy-2-phenethyl-1,2,3,4-tetrahydroisoquinoline substructure—is underway. Efficacy of these agents has been difficult to ascertain, partly due to a lack of pharmacokinetic reporters for quantifying inhibitor localization and transport dynamics. Some of the recent third generation inhibitors have a pendant heterocycle, for example, a chromone moiety, which we hypothesized could be converted to a fluorophore. Following synthesis and teasing of a small set of analogues, we identified one lead compound that can be used as a cellular imaging agent that exhibits structural similarity and behavior akin to the latest generation of MDR1 inhibitors.

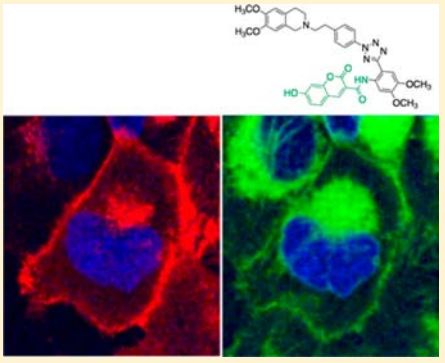

INTRODUCTION

Many cancers are resistant to or ultimately develop resistance to chemotherapeutic agents. One molecular mechanism of resistance is up-regulation of the membrane transporter multidrug resistance protein 1 (MDR1), also known as P-glycoprotein (permeability glycoprotein, P-gp), ATP-binding cassette subfamily B member 1 (ABCB1), or cluster of differentiation 243 (CD243).[1,2] During normal development, MDR1 plays a critical role in exporting xenobiotics from human tissues, particularly in the gut, liver, kidneys, and blood-brain barrier.[3,4] Many chemotherapeutics including taxanes, anthracyclines, and vinca alkaloids are substrates for MDR1,[5−7] and MDR1-induced multidrug resistance is a major cause of treatment failure in metastatic lung, breast, ovarian, cervical, and kidney cancers.[5,8−10]

One strategy for overcoming multidrug resistance is coadministration of an MDR1 inhibitor together with the primary chemotherapeutic agent. At least three generations of MDR1 inhibitors have been developed and tested clinically, with variable results.[11−14] First and second generation inhibitors such as verapamil, cyclosporin A, and valspodar failed in clinical trials due to dose-limiting toxicities and off-target effects.[14−16] A third generation of rationally designed inhibitors includes elacridar, zosuquidar, tariquidar, and HM30181 (Hanmi Pharmaceuticals);[10] these agents have been evaluated in clinical trials, but the results have been complex to interpret. In some cases, favorable safety profiles and encouraging patient responses were observed, but patient response rates have been unpredictable, conceivably due to heterogeneous MDR1 expression, coexpression of other efflux drug transporters (e.g., breast cancer resistance protein, BCRP) and other complicating factors.[5] Additionally, patient plasma concentrations of inhibitors often reach toxic levels before effective inhibitor concentrations are achieved at the tumor site.

We argue that there is a need for structurally matched imaging agents capable of real-time imaging of MDR1 expression and inhibition in single cells *in vivo*. Such an approach would shed light not only on the distribution of new inhibitors, but also their cellular effects over time. There is little knowledge regarding whether MDR1 inhibitors reach cells of interest and, if they do, over what time frame and with what level of heterogeneity. Similarly, there is limited *in vivo* knowledge regarding inhibitor activity and efficacy. Efficient strategies for cellular imaging of synthetic MDR1 inhibitors would elucidate all of these pharmacological parameters and be a useful tool for co-clinical trials.[17] Whereas some fluorescent substrates of MDR1 act as MDR1 inhibitors in a concentration-dependent manner (e.g., ^{99m}Tc-sestamibi, rhodamine 123), they generally have different chemical structures and *in vivo* behaviors compared to third generation MDR1 *modulators*, complicating analysis.[18] We therefore developed new fluorescent versions of a third generation MDR1 inhibitor to probe the intracellular behavior of the MDR1 inhibitor at the single cell level. Herein, we describe the synthesis of fluorescent analogues of anthranilamide-based third generation MDR1 modulators and disclose their photophysical properties and *in vitro* activities in a functional model of MDR1-induced paclitaxel resistance.

Received: April 8, 2014
Revised: May 6, 2014
Published: May 7, 2014

   dx.doi.org/10.1021/bc500154c | *Bioconjugate Chem.* 2014, 25, 1137−1142

RESULTS AND DISCUSSION

We sought to develop companion imaging agents for MDR1 inhibitors by making minor modifications to a parent third generation MDR1 inhibitor scaffold. Our lab has synthesized several companion imaging agents for subcellular applications including kinase inhibitors[19−21] and the poly(ADP-ribose)-polymerase inhibitor (PARPi) olaparib (AZD-2281).[22] In these cases, the parent inhibitors contained solvent-exposed auxiliary moieties, and the general strategy has involved converting a solvent-exposed group to a bioorthogonal handle (typically *trans*-cyclooctene) or appending a fluorophore (typically BODIPY, boron dipyrromethene). This strategy would be difficult to translate to the third generation acridine (e.g., elacridar)- or anthranilamide-based MDR1 inhibitors (Figure 1A); although the binding modes of these inhibitors are still unresolved, it is hypothesized that many third generation modulators bind to the same site as the MDR1 substrate Hoechst33342.[23] This binding site has no solvent-exposed sites, and several structure activity relationship (SAR) studies have revealed that addition of a large, hydrophobic substituent would cause a severe loss of function.[23] Moreover, appending a large moiety would increase the lipophilicity and molecular weight, which could not only reduce the inhibitory activity, but also render the molecule a *substrate* for MDR1.[24] This problem was observed when the MDR1 modulator verapamil was modified with a BODIPY substituent, making verapamil-BODIPY an ineffective probe for studying MDR1 *inhibitor* dynamics.[25]

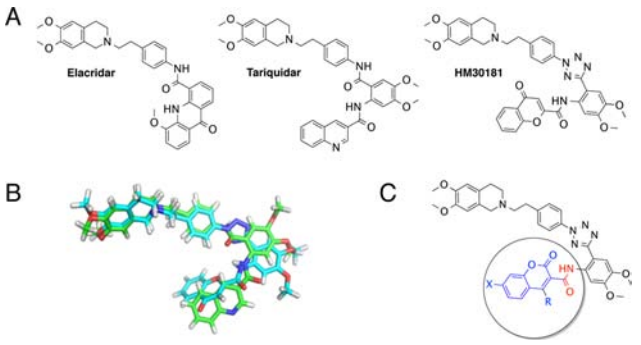

Figure 1. (A) Representative third generation MDR1 inhibitors. (B) Flexible overlay of tariquidar and HM30181 (generated using Forge software package, Cresset, United Kingdom). (C) General strategy for introduction of fluorophores to the HM30181 scaffold.

Tariquidar and its tetrazole-containing analogue, HM30181,[10,26] were chosen as representative third generation modulators due to the presence of an anthranilic acid portion that could be derivatized from a common aniline intermediate. The compounds also share a common pharmacophore (Figure 1B) in their native configuration. We chose the HM30181 scaffold because this inhibitor has a chromone at the proposed amide modification site. Some chromone (4*H*-chromen-4-one) derivatives are fluorescent (e.g., flavones), but HM30181 exhibits little to no fluorescence when excited in the UV−vis range. Given that exchanging a chromone (4*H*-chromen-4-one) for a fluorescent coumarin (2*H*-chromen-2-one) would incur little change in terms of molecular weight and overall structure, we generated a small library of derivatives based on this exchange (Figure 1C).

Synthesis of analogues **2**−**6** was accomplished with standard amide-bond forming reactions using known aniline **1** as a starting material (Scheme 1). For the synthesis of 7-hydroxycoumarins **4** and **6**, the requisite carboxylic acids were first converted to the corresponding acetates prior to coupling. In these cases, mixtures of both acetylated and deacetylated coumarin products were obtained (as evidenced by LCMS analysis of the crude mixtures), and the deacetylated coumarins (i.e., **4** and **6**) were isolated for further study.

The analogues were evaluated for inhibitory efficacy using a parent HT1080 cell line that is highly sensitive to taxanes; its resistant analogue (MDR1++) was generated via stable transfection of the MDR1 gene using a Lentiviral expression system. Inhibitory efficacy was determined by resensitization of MDR1++ cells to paclitaxel (Table 1 and Figure 2). As expected, HM30181 reversed the multidrug resistant phenotype, making the MDR1++ cell line sensitive, akin to the parent line, at concentrations between 100 nM and 500 nM (Supporting Information). Higher concentrations of the fluorescent analogues were necessary to recover sensitivity. HM30181 analogues were compared according to the EC_{50} values of paclitaxel when coadministered with 5 μM concentrations of inhibitor analogues (Table 1). We also

Scheme 1. (A) Synthesis of HM30181 Analogues via a Chromone to Coumarin Substitution. (B) Synthesis of BODIPY-Analogue 7. (C) Synthesis of Negative Control 8

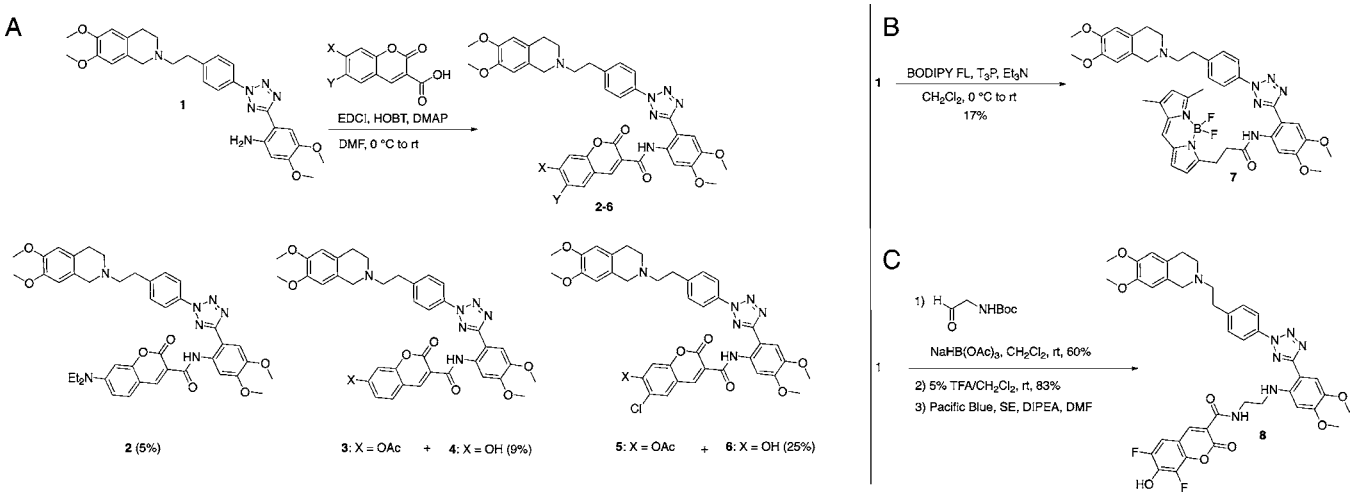

dx.doi.org/10.1021/bc500154c | *Bioconjugate Chem.* 2014, 25, 1137−1142

Table 1. In Vitro Activity Profiles and Photophysical Properties of HM30181 and Fluorescent Analogues

compound	EC_{50}[paclitaxel], nM (95% CI)[a]	surviving fraction[b]	λ (nm) Abs/Em[c]	ϕ[d]
HM30 181	2.3 (1.6–3.4)[e]	5%	NA[f]	NA
2	13.5 (10.0–18.4)	10%	435/486	0.027
4	18.6 (9.0–38.3)	10%	427/454	0.090
6	353 (192–941)	48%	432/456	ND
7	66.5 (46.2–95.5)	24%	509/517	ND
8	>1000	NA	416/447	ND

[a]EC_{50} values represent the concentration of paclitaxel required to induce cell death in paclitaxel- resistant HT1080 cells when used in combination with 5 μM HM30181 or HM30181 analogues. See the Supporting Information for dose–response plots showing inhibitor efficacy against both the paclitaxel-sensitive and -resistant cell lines. [b]Percentage of the cell population surviving at the maximum dose of paclitaxel (1 μM). [c]Wavelength at maximal (relative) absorbance and fluorescence emission in PBS (pH 7.4) using compound concentrations of 10 μM. [d]Quantum yields were determined for the test compounds in PBS (pH 7.4) using coumarin-153 in EtOH as a standard (λ Ex = 410 for **2** and 405 for **4**, respectively). All measurements were performed in triplicate. [e]HM30181 induces reversal of paclitaxel resistance at much lower concentrations than 5 μM. The EC_{50} values for paclitaxel were 4.4 and 5.4 nM at 1 μM and 500 nM concentrations of HM30181, respectively. [f]HM30181 has absorbance bands ranging from 290 to 450 nm, but no fluorescence was observed when solutions of HM30181 were excited at these wavelengths.

studied the photophysical properties of the new compounds to choose the best candidate for intracellular imaging.

Compounds wherein the chromone moiety was exchanged for a coumarin exhibited varying levels of inhibitory activity (Table 1). We used 7-diethylaminocoumarin derivative **2** as a starting structure because it showed promising inhibitory activity at 5 μM concentrations; however, **2** also exhibited limited aqueous solubility, a low quantum yield (Table 1, entry 2), and a red-shifted emission spectrum (Supporting Information), which could complicate multichannel imaging analyses. By changing the substitution at the 7-position from the diethylamino- group to a hydroxy- group, we generated derivative **4**, which was more soluble in PBS, had an improved quantum yield (Table 1), and still maintained potency for reversing taxol resistance. Moreover, the inhibitory activity was maintained at lower inhibitor concentrations (Figure 2). We reasoned that introduction of a chloro-substituent adjacent to the hydroxy-group (i.e., compound **6**) would further improve fluorescence properties (e.g., quantum yield) while maintaining inhibitor potency; yet, surprisingly, a significant drop in inhibitory activity was observed (Table 1). It should be noted that these inhibitor analogues do not induce cell death in either paclitaxel-sensitive or -resistant cell lines in the absence of paclitaxel (Supporting Information).

The BODIPY-FL derivative **7** was synthesized to ascertain whether we could, in fact, make a brighter imaging agent while maintaining potency (Scheme 1B). Surprisingly, the BODIPY FL-substituted derivative still showed modest activity when applied at 5 μM concentrations; however, analogue **7** exhibited poor aqueous solubility, limiting its use in cellular imaging applications. As a negative control for the paclitaxel resensitization assay, we synthesized analogue **8** (Scheme 1C). It has been established that a hydrogen-bonding accepting moiety such as the amide *ortho*- to the tetrazole in HM30181 is essential for maintaining MDR1 inhibitory activity.[27] Consistent with established pharmacophore models of third generation MDR1 modulators, this derivative was not active for reversing the phenotype of the paclitaxel-resistant cell lines (Table 1). It is also possible that the more acidic Pacific Blue coumarin renders this compound impermeable to cell membranes at physiological pH; the lack of inhibitory activity exhibited by compound **8** indicates either the importance of pharmacophore, importance of membrane permeability, or a combination of the two factors.

Based on the collective data regarding inhibitory activities and photophysical properties, the 7-hydroxycoumarin derivative **4** was chosen for use in cellular imaging experiments. The probe was applied to a mixed population of parent (paclitaxel-sensitive) and MDR1++ (paclitaxel-resistant) HT1080 cells expressing fluorescent histone markers (Figure 3). Accumulation of HM30181–7HC in MDR1++ cells was consistent with that in the parent HT1080 cells, indicating that derivative **4** is not a substrate (i.e., does not get effluxed) of the MDR1 membrane transport protein. Probe **4** showed colocalization

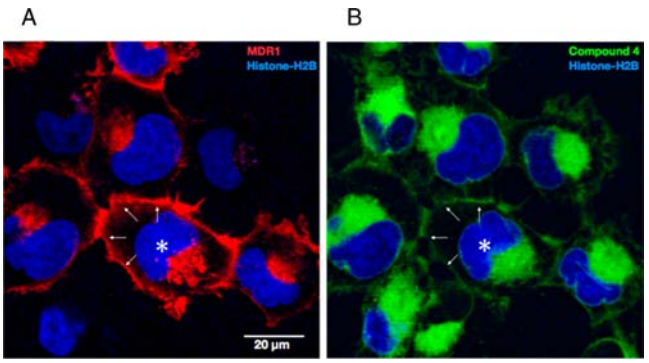

Figure 3. Cellular localization of analogue **4** in a mixed population of paclitaxel-sensitive and paclitaxel-resistant cell lines. (A) MDR1-apple (red) and histone-H2B-iRFP (blue). (B) Compound **4** (green) and histone-H2B-iRFP (blue).

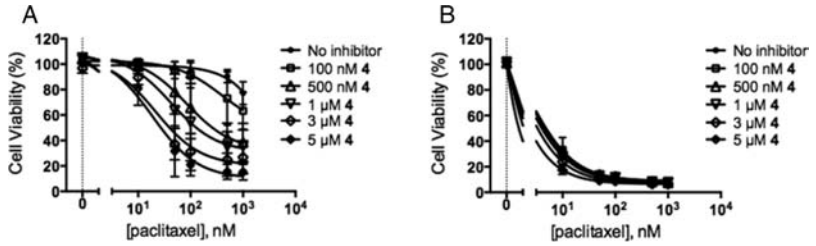

Figure 2. Representative data from a paclitaxel resensitization assay: cellular activity profile of analogue **4** in (A) paclitaxel-resistant and (B) paclitaxel-sensitive HT1080 cell lines.

dx.doi.org/10.1021/bc500154c | *Bioconjugate Chem.* 2014, 25, 1137–1142

with MDR1 in MDR1++ cells, but **4** was also observed in the endoplasmic reticulum and the perinuclear space.

To visualize the function of compound **4**, we studied the cellular uptake of the Poly-ADP ribose polymerase inhibitor olaparib-BFL (olaparib modified with a BODIPY substituent). Olaparib is a known MDR1 substrate,[28] and olaparib-BFL has been validated as a viable companion imaging agent for studying cellular distribution of this inhibitor.[22,29] Mixed populations of parent and MDR1++ HT1080 cells were treated with olaparib-BFL in the absence of inhibitor; as depicted in Figure 4, olaparib-BFL accumulates in the nucleus of the parent

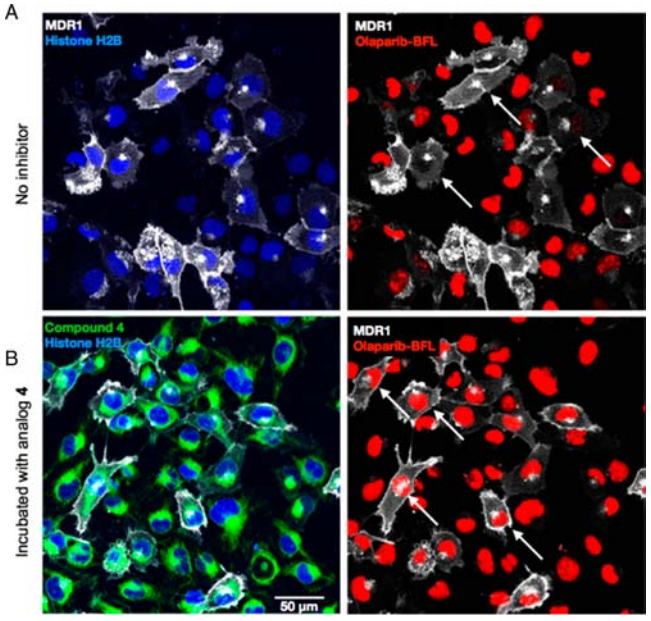

Figure 4. Cellular uptake of olaparib-BFL in paclitaxel-sensitive and paclitaxel-resistant cell lines (A) in the absence of analogue **4** and (B) after coincubation of olabarib-BFL with analogue **4**. MDR1 (white); histone-H2B-iRFP (blue); compound **4** (green); olaparib-BFL (red).

cells but is not present in the MDR1++ cells. When cells were treated with **4**, cellular uptake of Olaparib-BFL was observed in both the parent and MDR1++ cells. Beyond excellent colocalization (Figure 3), and demonstration of drug efflux reversal (Figure 4), the specificity of this analogue was demonstrated by competition of **4** with surplus HM30181; preincubation with HM30181 blocked uptake of compound **4** by approximately 80% (Figure 5).

Multidrug resistance, whereby patients become refractory to a broad spectrum of structurally unrelated compounds, is often implicated in the failure of chemotherapy regimens and eventual tumor progression. The rationale for developing MDR1 inhibitors is thus sound, but unfortunately, several classes of compounds have repeatedly failed in clinical trials. The specific reasons for these failures remain unclear; therefore, tools for quantifying the pharmacokinetic and pharmacodynamic properties of new MDR1 inhibitors are necessary.

Clinical imaging agents used to measure MDR1 activity have been difficult to interpret and do not provide single cell resolution. One of the more commonly used agents, ^{99m}Tc sestamibi, originally developed for other applications but subsequently shown to be an MDR1 substrate,[30] is detected by nuclear imaging technologies that are limited in resolution by volume averaging and ratio imaging. At the cellular level,

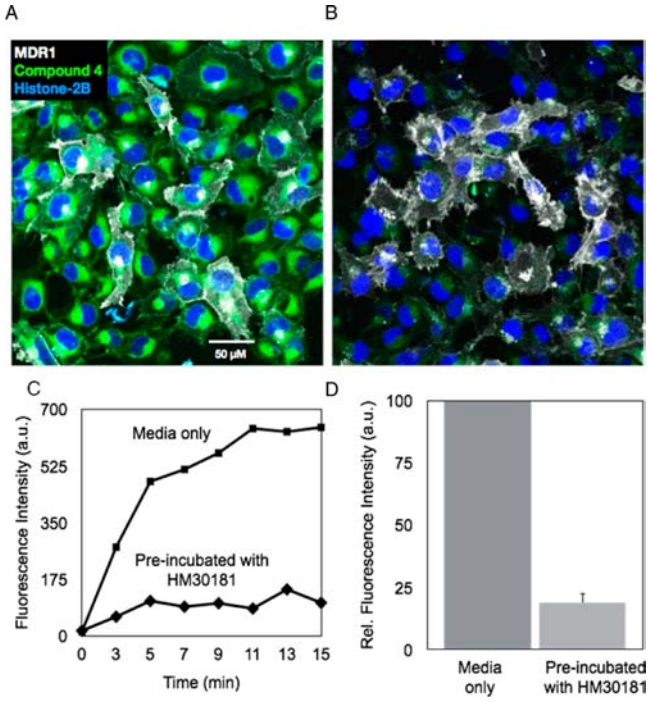

Figure 5. Inhibition of cellular uptake of analogue **4** via preincubation with HM30181. (A) A mixed population of paclitaxel-sensitive and -resistant cell lines was preincubated with media only, and the media was replaced with media containing analogue **4** (3 μM) (control). (B) The mixed population was pretreated with HM30181 (30 μM) prior to exchanging the media for media with analogue **4** (3 μM) (pretreated). (C) Fluorescence intensity from probe **4** observed over time in control and pretreated cell populations. (D) Averaged relative fluorescence intensity of control and pretreated cell populations.

other fluorochromes are commonly used as substrates to estimate MDR1 activity.[31−33] These probes, however, have different structural compositions compared to third generation MDR1 inhibitors and are not specific transport modulators. In contrast, the system described herein demonstrates quantification of MDR1 substrate and modulator activity in parallel and at single cell resolution. Exquisite channel separation was achieved for simultaneous visualization of multiple components of a complex system; the real-time distribution of two small molecules (MDR1 substrate, MDR1 inhibitor) in conjunction with visualization of the target protein (via fluorescent expression of MDR1) and the cell nucleus (histone markers) was demonstrated.

Derivative **4** should prove to be a useful tool for in vivo real-time monitoring of MDR1 modulators in tandem with a suitable MDR1 substrate and, potentially, for assessing efficacy of vehicles for delivery of MDR1 modulators. These projected studies will provide insight into the pharmacokinetics and pharmacodynamics of MDR1 inhibitors in vivo and allow for optimization of combination therapies (strategy for dual administration of MDR1i with primary chemotherapeutic). Use of probe **4** or a related companion imaging agent could have broad implications for the design of future MDR1 inhibitors.

■ ASSOCIATED CONTENT

Ⓢ Supporting Information

Procedures for chemical synthesis, compound characterization data, fluorescence spectra, procedures for quantum yield

dx.doi.org/10.1021/bc500154c | *Bioconjugate Chem.* 2014, 25, 1137−1142

determinations, procedures for cell line construction, Western blot, and cell viability assays, in vitro activity toward BCRP modulation, and additional imaging data. This material is available free of charge via the Internet at http://pubs.acs.org.

AUTHOR INFORMATION

Corresponding Author

*Phone: 617-726-8226. E-mail: rweissleder@mgh.harvard.edu.

Author Contributions

Melissa M. Sprachman and Ashley M. Laughney contributed equally to this work.

Notes

The authors declare no competing financial interest.

ACKNOWLEDGMENTS

M.M.S. and A.M.L. were supported by a NIH grant T32-CA079443. We are grateful to Dr. Sarit Agasti for helpful discussions and the kind gift of 6-chloro-7-hydroxycoumarin-3-carboxylic acid; Dr. Ralph Mazitschek for computational modeling of the tariquidar and HM30181 structure overlays; and Dr. Jonathan Carlson, Dr. Labros Meimitis, and Dr. Eunha Kim for many helpful discussions.

ABBREVIATIONS

EDCI, 1-ethyl-3-(3-(dimethylamino)propyl)carbodiimide; HOBT, *N*-hydroxybenzotriazole; DMAP, 4-dimethylaminopyridine; DMF, *N*,*N*-dimethylformamide; BODIPY FL, 7-(2-carboxyethyl)-5,5-difluoro-1,3-dimethyl-5*H*-dipyrrolo[1,2-*c*:2′,1′-*f*][1,3,2]diazaborinin-4-ium-5-uide; T_3P, propylphosphonic anhydride; Boc, *tert*-butyloxycarbonyl; TFA, trifluoroacetic acid; Pacific Blue, SE, 6,8-difluoro-7-hydroxy-2-*oxo*-2*H*-chromene-3-carboxylic acid, succinimidyl ester; DIPEA, *N*,*N*-diisopropylethylamine

REFERENCES

(1) Borst, P., and Schinkel, A. H. (2013) P-glycoprotein ABCB1: A major player in drug handling by mammals. *J. Clin. Invest. 123*, 4131–4133.

(2) Kunjachan, S., Rychlik, B., Storm, G., Kiessling, F., and Lammers, T. (2013) Multidrug resistance: Physiological principles and nanomedical solutions. *Adv. Drug Delivery Rev. 65*, 1852–1865.

(3) Misaka, S., Muller, F., and Fromm, M. F. (2013) Clinical relevance of drug efflux pumps in the gut. *Curr. Opin. Pharmacol. 13*, 847–852.

(4) Deeley, R. G., Westlake, C., and Cole, S. P. (2006) Transmembrane transport of endo- and xenobiotics by mammalian ATP-binding cassette multidrug resistance proteins. *Physiol. Rev. 86*, 849–899.

(5) Colabufo, N. A., Berardi, F., Cantore, M., Contino, M., Inglese, C., Niso, M., and Perrone, R. (2010) Perspectives of P-glycoprotein modulating agents in oncology and neurodegenerative diseases: pharmaceutical, biological, and diagnostic potentials. *J. Med. Chem. 53*, 1883–1897.

(6) Nobili, S., Landini, I., Mazzei, T., and Mini, E. (2012) Overcoming tumor multidrug resistance using drugs able to evade P-glycoprotein or to exploit its expression. *Med. Res. Rev. 32*, 1220–1262.

(7) Aller, S., Yu, J., Ward, A., Weng, Y., Chittaboina, S., Zhuo, R., Harrell, P. M., Trinh, Y. T., Zhang, Q., Urbatsch, I. L., and Chang, G. (2009) Structure of P-glycoprotein reveals a molecular basis for poly-specific drug binding. *Science 323*, 1718–1722.

(8) Mechetner, E., Kyshtoobayeva, A., Zonis, S., Kim, H., Stroup, R., Garcia, R., Parker, R. J., and Fruehauf, J. P. (1998) Levels of multidrug resistance (MDR1) P-glycoprotein expression by human breast cancer correlate with in vitro resistance to taxol and doxorubicin. *Clin. Cancer Res. 4*, 389–398.

(9) Longley, D. B., and Johnston, P. G. (2005) Molecular mechanisms of drug resistance. *J. Pathol. 205*, 275–292.

(10) Kwak, J. O., Lee, S. H., Lee, G. S., Kim, M. S., Ahn, Y. G., Lee, J. H., Kim, S. W., Kim, K. H., and Lee, M. G. (2010) Selective inhibition of MDR1 (ABCB1) by HM30181 increases oral bioavailability and therapeutic efficacy of paclitaxel. *Eur. J. Pharmacol. 627*, 92–98.

(11) McDevitt, C. A., and Callaghan, R. (2007) How can we best use structural information on P-glycoprotein to design inhibitors? *Pharmacol. Ther. 113*, 429–441.

(12) Yang, K., Wu, J., and Li, X. (2008) Recent advances in research on P-glycoprotein inhibitors. *BioScience Trends 2*, 137–146.

(13) Zhang, L., and Ma, S. (2010) Efflux pump inhibitors: a strategy to combat P-glycoprotein and the NorA multidrug resistance pump. *ChemMedChem 5*, 811–822.

(14) Nieto Montesinos, R., Beduneau, A., Pellequer, Y., and Lamprecht, A. (2012) Delivery of P-glycoprotein substrates using chemosensitizers and nanotechnology for selective and efficient therapeutic outcomes. *J. Controlled Release 161*, 50–61.

(15) Raderer, M., and Scheithauer, W. (1993) Clinical trials of agents that reverse multidrug resistance. A literature review. *Cancer 72*, 3553–3563.

(16) Krishna, R., and Mayer, L. D. (2000) Multidrug resistance (MDR) in cancer. Mechanisms, reversal using modulators of MDR and the role of MDR modulators in influencing the pharmacokinetics of anticancer drugs. *Eur. J. Pharm. Sci. 11*, 265–283.

(17) Chen, Z., Cheng, K., Walton, Z., Wang, Y., Ebi, H., Shimamura, T., Liu, Y., Tupper, T., Ouyang, J., Li, J., Gao, P., Woo, M. S., Xu, C., Yanagita, M., Altabef, A., Wang, S., Lee, C., Nakada, Y., Pena, C. G., Sun, Y., Franchetti, Y., Yao, C., Saur, A., Cameron, M. D., Nishino, M., Hayes, D. N., Wilkerson, M. D., Roberts, P. J., Lee, C. B., Bardeesy, N., Butaney, M., Chirieac, L. R., Costa, D. B., Jackman, D., Sharpless, N. E., Castrillon, D. H., Demetri, G. D., Janne, P. A., Pandolfi, P. P., Cantley, L. C., Kung, A. L., Engelman, J. A., and Wong, K. K. (2012) A murine lung cancer co-clinical trial identifies genetic modifiers of therapeutic response. *Nature 483*, 613–617.

(18) Saneja, A., Khare, V., Alam, N., Dubey, and Gupta, P. M. D. (2014) Advances in P-glycoprotein-based approaches for delivering anticancer drugs: pharmacokinetic perspective and clinical relevance. *Expert Opin. Drug Delivery 11*, 121–138.

(19) Budin, G., Yang, K. S., Reiner, T., and Weissleder, R. (2011) Bioorthogonal probes for polo-like kinase 1 imaging and quantification. *Angew. Chem., Int. Ed. Engl. 50*, 9378–9381.

(20) Yang, K. S., Budin, G., Reiner, T., Vinegoni, C., and Weissleder, R. (2012) Bioorthogonal imaging of aurora kinase A in live cells. *Angew. Chem., Int. Ed. Engl. 51*, 6598–6603.

(21) Kim, E., Yang, K. S., and Weissleder, R. (2013) Bioorthogonal small molecule imaging agents allow single-cell imaging of MET. *PLoS One 8*, e81275.

(22) Thurber, G. M., Yang, K. S., Reiner, T., Kohler, R. H., Sorger, P., Mitchison, T., and Weissleder, R. (2013) Single-cell and subcellular pharmacokinetic imaging allows insight into drug action in vivo. *Nat. Commun. 4*, 1504.

(23) Globisch, C., Pajeva, I. K., and Wiese, M. (2006) Structure-activity relationships of a series of tariquidar analogs as multidrug resistance modulators. *Bioorg. Med. Chem. 14*, 1588–1598.

(24) Chang, C., Bahadduri, P. M., Polli, J. E., Swaan, P. W., and Ekins, S. (2006) Rapid identification of P-glycoprotein substrates and inhibitors. *Drug Metab. Dispos. 34*, 1976–1984.

(25) Crivellato, E., Candussio, L., Rosati, A. M., Bartoli-Klugmann, F., Mallardi, F., and Decorti, G. (2002) The fluorescent probe Bodipy-FL-verapamil is a substrate for both P-glycoprotein and multidrug resistance-related protein (MRP)-1. *J. Histochem. Cytochem. 50*, 731–734.

(26) Bang, K. C., Cha, M. Y., Ahn, Y. G., Ham, Y. J., Kim, M. S., and Lee, G. S. (2005) P-Glycoprotein Inhibitor, Method for Preparing the Same and Pharmaceutical Composition Comprising the Same, PCT Int. Appl. WO 2005/033097 A1.

(27) Pajeva, I. K., Sterz, K., Christlieb, M., Steggemann, K., Marighetti, F., and Wiese, M. (2013) Interactions of the multidrug resistance modulators tariquidar and elacridar and their analogues with P-glycoprotein. *ChemMedChem 8*, 1701−1703.
(28) Rottenberg, S., Jaspers, J. E., Kersbergen, A., van der Burg, E., Nygren, A. O. H., Zander, S. A. L., Derksen, P. W. B., de Bruin, M., Zevenhoven, J., Lau, A., Boulter, R., Cranston, A., O'Connor, M. J., Martin, N. M. B., Borst, P., and Jonkers, J. (2008) High sensitivity of BRCA1-deficient mammary tumors to the PARP inhibitor AZD2281 alone and in combination with platinum drugs. *Proc. Natl. Acad. Sci. U.S.A. 105*, 17079−17084.
(29) Reiner, T., Lacy, J., Keliher, E. J., Yang, K. S., Ullal, A., Kohler, R. H., Vinegoni, C., and Weissleder, R. (2012) Imaging therapeutic PARP inhibition *in vivo* through bioorthogonally developed companion imaging agents. *Neoplasia 14*, 169−177.
(30) Dizdarevic, S., and Peters, A. M. (2011) Imaging of multidrug resistance in cancer. *Cancer Imaging 11*, 1−8.
(31) Lebedeva, I. V., Pande, P., and Patton, W. F. (2011) Sensitive and specific fluorescent probes for functional analysis of the three major types of mammalian ABC transporters. *PLoS One 6*, e22429.
(32) Zolnerciks, J. K., Booth-Genthe, C. L., Gupta, A., Harris, J., and Unadkat, J. D. (2011) Substrate- and species-dependent inhibition of P-glycoprotein-mediated transport: implications for predicting in vivo drug interactions. *J. Pharm. Sci. 100*, 3055−3061.
(33) Strouse, J. J., Ivnitski-Steele, I., Waller, A., Young, S. M., Perez, D., Evangelisti, A. M., Ursu, O., Bologa, C. G., Carter, M. B., Salas, V. M., Tegos, G., Larson, R. S., Oprea, T. I., Edwards, B. S., and Sklar, L. A. (2013) Fluorescent substrates for flow cytometric evaluation of efflux inhibition in ABCB1, ABCC1, and ABCG2 transporters. *Anal. Biochem. 437*, 77−87.